Brief report of SWEA EM preliminary calibration.

Andrei Fedorov, Jean-Louis Medale, Jean Rouzaud, Jean-Andre Sauvaud and Thomas Moreau

Centre d'Etude Spatiale des Rayonnements

1. Calibration set-up. Coordinate system, terms, and technical details.

Sensor configuration, set-up and coordinates are shown in figure 1. Only 90° of 360° azimuthal field of view is under the entrance grid stack. Amplifiers are connected to the 7 shadowed anode sectors only. The mechanical set-up allows to turn the electron beam around the sensor for ±180° in elevation (polar) plane, but the beam turns for ±15° only in azimuthal plane. Thus during calibration only sectors # 3, 4, and then # 11 have been illuminated. The electronic set-up is shown in the low panel of figure 1. DAC has a 2mV resolution. The correspondence of reference, high voltage, and housekeeping values is as follows:

$$UanHV[V] = -0.1502\ UanRef[mV] + 0.36$$

$$UanHV[V] = 0.1688\ Uanhk[mV] + 0.36$$

$$UdefTHV[V] = -0.7532\ UdefTref[mV] + 4.368$$

$$UdefTHV[V] = 0.3200\ UdefThk[mV] + 4.457$$

$$UdefBHV[V] = -0.7496\ UdefBref[mV] + 2.426$$

$$UdefBHV[V] = 0.3293\ UdefBhk[mV] + 2.222$$

$$MCPHV[V] = -0.6937\ UMCPref[mV] + 1.15$$

$$MCPHV[V] = 0.993\ UMCPhk[mV] + 1.348$$

Because the earth's magnetic field is not compensated in the vacuum chamber, the minimal energy of electron beam is 2000eV. The electron gun keeps the beam intensity constant with accuracy of about 2%. The center of rotation of the sensor in the elevation plane lies at the axis of the sensor symmetry, thus during rotation, the center of the beam moves from the real entry point. To avoid the effect of beam non-homogeneity, the sensor sis hifted according to:

$$dZ[mm] = \pm(-0.104 + 0.644\ Elev[deg] - 0.0013\ Elev[deg]^2)$$

Here dZ is vertical shift, and $Elev$ is elevation angle of the beam. The previous formula has been derived from the numerical ray-tracing. The photo of the installation is shown in figure 2

2. MCP characterization.

Before the real calibration the detector part of the sensor (MCP, anode, anode electronics, and HV electronics) has been placed under the electron beam to characterize the MCP stack and amplifiers. The sketch of the set-up is presented in figure 3. Figure 4 shows the anode sectors count versus $UMCPhk$. All profiles have been normalized to the saturating count of the anode # 1. Starting with $UMCPhk = 2700mV$ count of all sectors is saturated. The sensor calibration have been performed just at this MCP bias. Extra information comes from the pulse-height analysis. Figure 5 shows the gain distribution for 4 selected sectors. One can see that the gain varies from channel to channel not more than 35%. The threshold has been set equal to $3 \cdot 10^5$ for all amplifiers.$3 \cdot 10^5$.

3. Instrument response. Terms definition.

Before discussion on calibration results we need to define several terms. There are two invariant values which control the trajectories inside deflector and top-hat analyzer. Namely:

$$K = E/Uan$$

and

$$D = (UdefT - UdefB)/E$$

Here E is the incident electron energy, eV. If incident azimuth is constant, the entire response of a sensor is 3-D function

$$A = f(K, D, Elev)$$

Here A is the effective aperture of a sensor. The shape of this function is shown in figure 6, left panel. It looks like a tube which increases the mean value of $Elev$ with D, and keeps the mean value of K nearly constant. Note, that particular response of the instrument with fixed $UdefB$, $UdefT$, and Uan is the cross-section of the tube $f(K, D, Elev)$ by plane $D \cdot K = const$. The projection of the entire response to the plane {D, Elev}, namely $\int f(K, D, Elev)dK$ is shown in the right panel of figure 6. The profile of the local maximum of this function is almost straight line. Let dEl/dD is the local derivative of the the maximum profile. Because of the function $\int f(K, D, Elev)dK$ is "thin" and the its contours are mostly parallel to the maximum profile, we can re-calculate response $A = f(K, D, Elev0 = const)$ to response $A = f(K, D0 = const, Elev)$ by formula

$$(Elev - Elev0) = -\frac{dElev}{dD}(D - D0)$$

4. Analyzer response and grid transparency.

Figure 7 shows the energy-elevation response of two azimuthal sectors: # 3 (under the grid) and # 11 (without grid). In both cases the azimuth of the beam was at the middle of the sector. Two responses are generally similar, but the response of sector # 11 is a little bit wider in elevation, as well as in the energy space. Probably the grid can limit the

width of the response. The transparency of the grid is estimated from the comparison of the total count of two sectors (the beam intensity has been kept constant). The measured transparency for zero central elevation (deflector is OFF) is 65%.

5. Azimuthal resolution.

Figure 8 shows the azimuthal response of two anode sectors. At the each azimuthal point the full energy-elevation response was taken and then integrated. The azimuthal resolution is close to the expected one, but there is some $\sim 1\%$ "tail" when the beam is in the middle of the next sector. The value of this "tail" decreases with azimuth, hence it is not cross-talk. Probably it is effect of scattering of electrons passing by glance trajectories at the grid crosspieces.

6. Deflector properties.

To diminish the number of mechanical turn, the deflector properties have been measured as follows: the elevation angle was mechanically set in $Elev0$ position (from $-65°$ up to $+65°$ with step $5°$), and the $D-K$ scanning was made. In order to simulate the energy scan, $(UdefT - UdefB)/Uan = D \cdot K = D_i \cdot K0 = const$ for each specified D_i from the range around $D0$ theoretically corresponding to $Elev0$. Then each value of D has been re-calculated to the current virtual elevation. Figure 9a shows the projection of the sensor response to the D - $Elev$ (real mechanical elevation!) plane integrated over the K range. The azimuthal angle has been set equal to $14°$. Due to minimal beam energy of 2000eV the $D - Elev$ response is cut off at the value ± 0.7. Because of the finite width of D - $Elev$ response the measurements with $Elev > 55°$ and $Elev < -50°$ are not representative. The function $Elev(D)$ is very linear:

$$Elev = 2.27 + 85.11\ D$$

Figure 9b presents response in $Elev - K$ space. Note that here $Elev$ is re-calculated from D. Finally figure 10 shows the elevation response around each $Elev0$ position. The red profile shows the total count (like $< Geometrical factor > /\Delta Az$). One can see that there is no significant degradation of the grid transparency with elevations, but there is clear asymmetry between negative and positive elevations. The angular resolution about $10°$ is close to the theoretically expected.

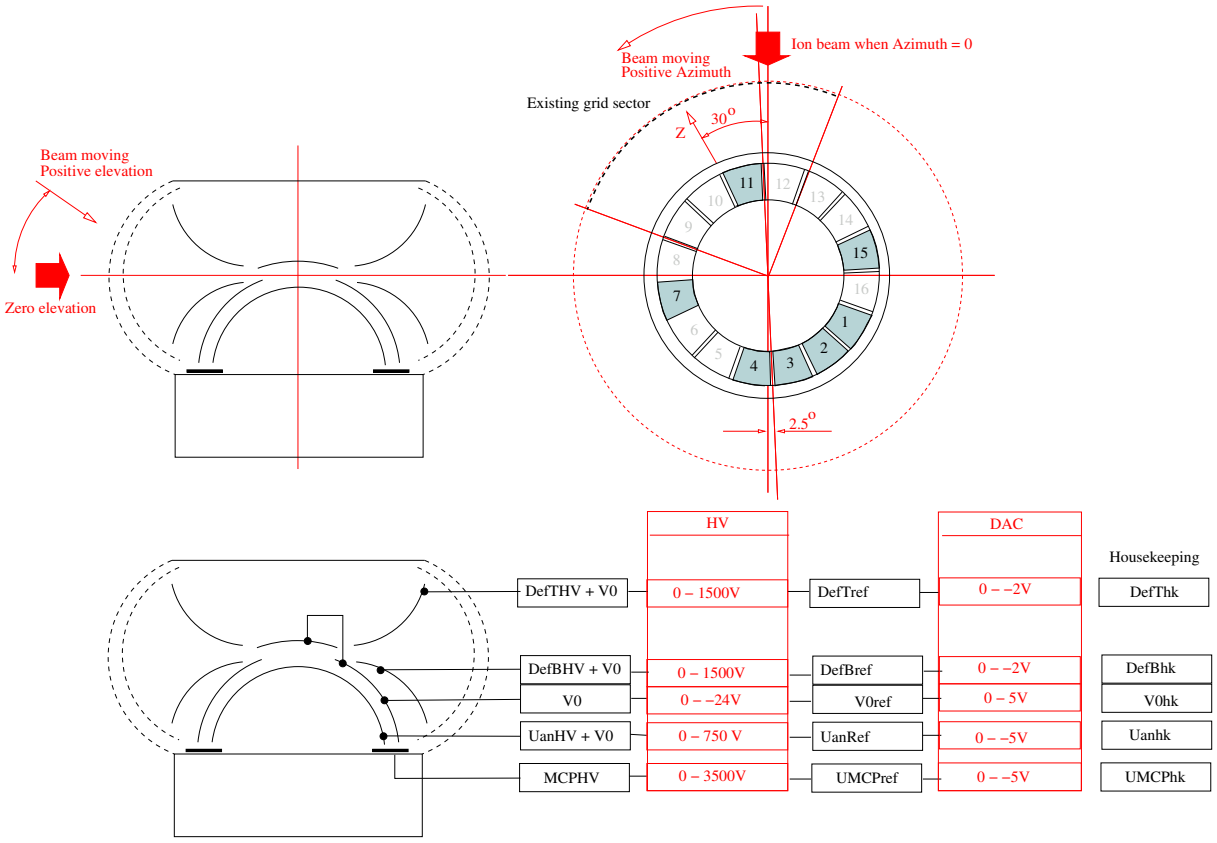

Figure 1: The instrument set-up. Top two panels show the electron beam coordinates, existing grid position and working sectors of the anode (shadowed). The low panel shows high voltage notification and voltage ranges.

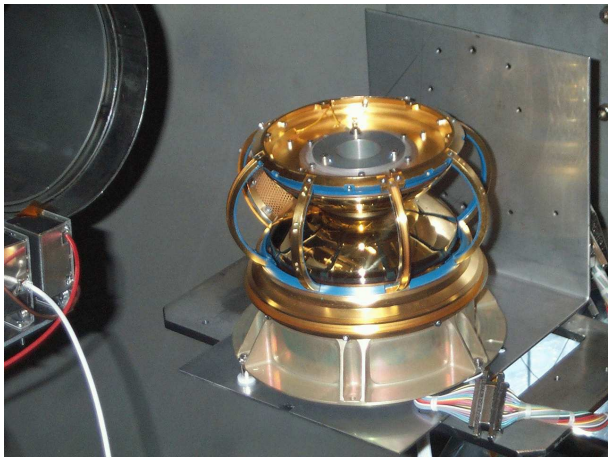

SWEA EM in the vacuum chamber

Figure 2: The sensor in the vacuum chamber.

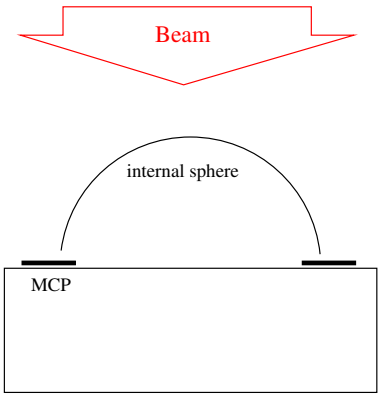

Figure 3: Set-up for MCP characterization.

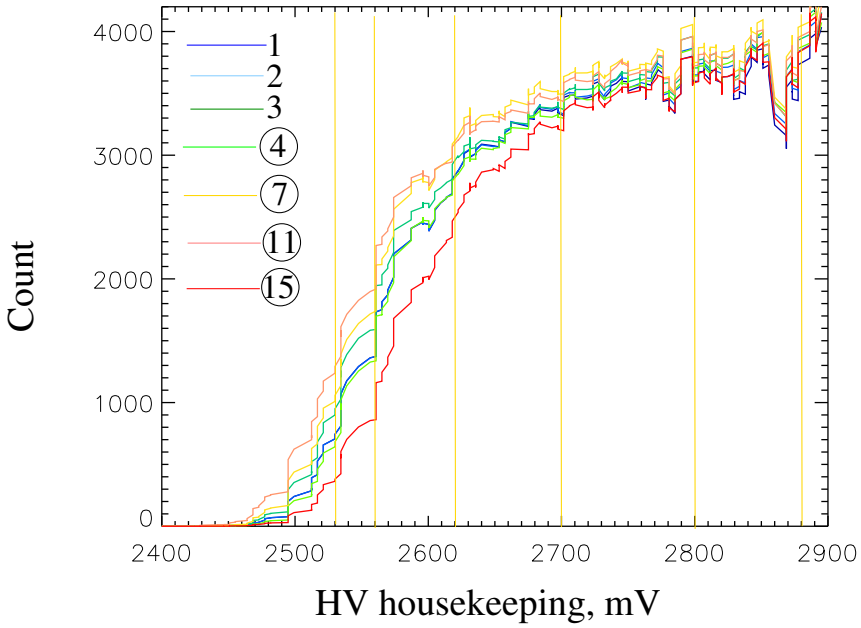

Figure 4: Sectors count versus monitor value of MCP voltage. The pulse height analysis (see figure 5) has been made for rounded sectors.

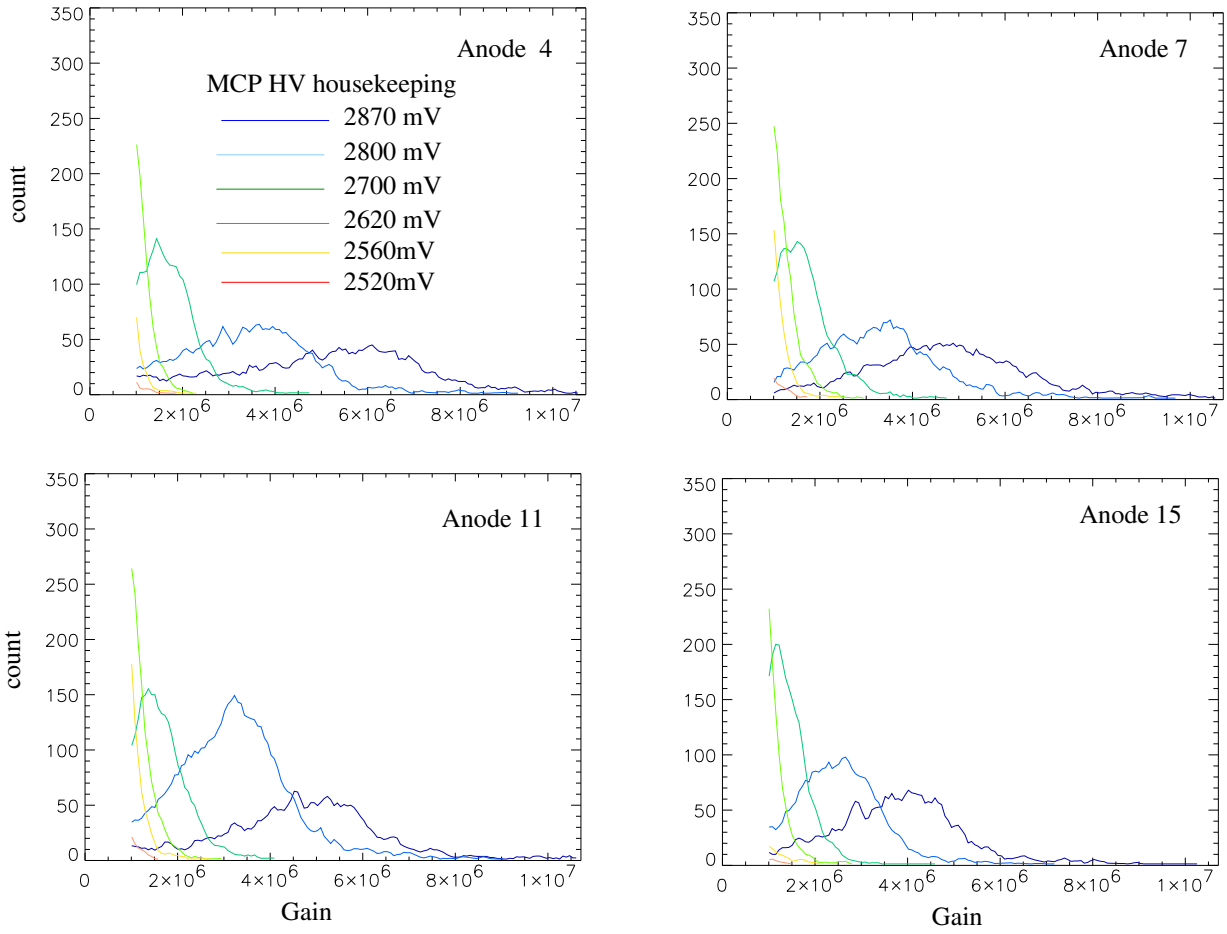

Figure 5: The pulse height distribution for 4 selected azimuthal sectors. The pals amplitude is given in electron charges.

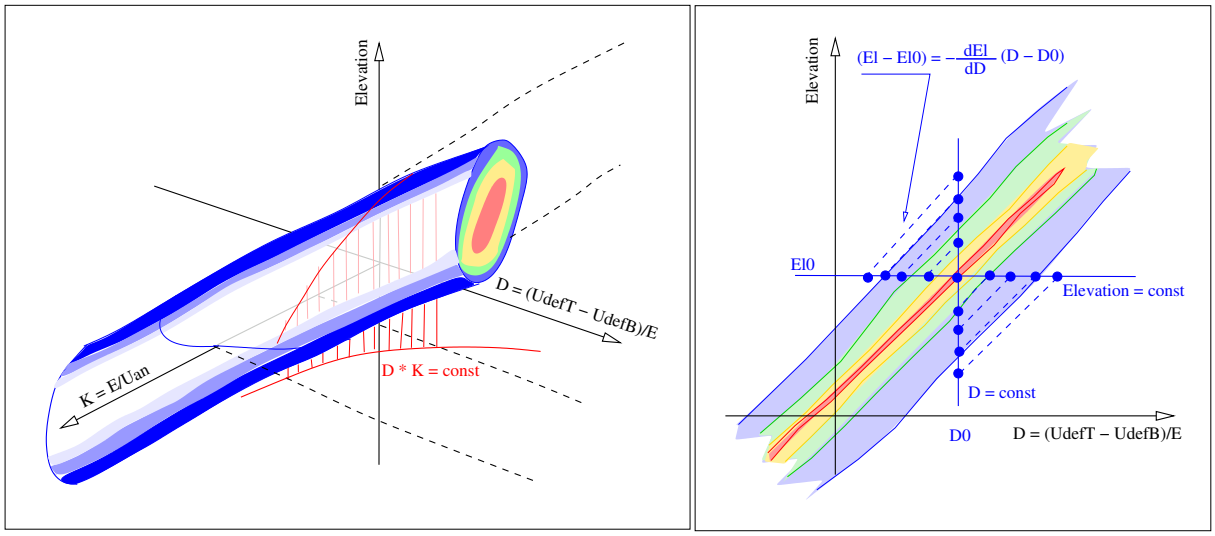

Figure 6: Left panel: Diagram showing the shape of a sensor response for constant azimuth. See text for details. Right panel: projection of a sensor response onto {D,Elevation} plane. The dashed lines shows the reconstruction of the elevation response from the "D" response.

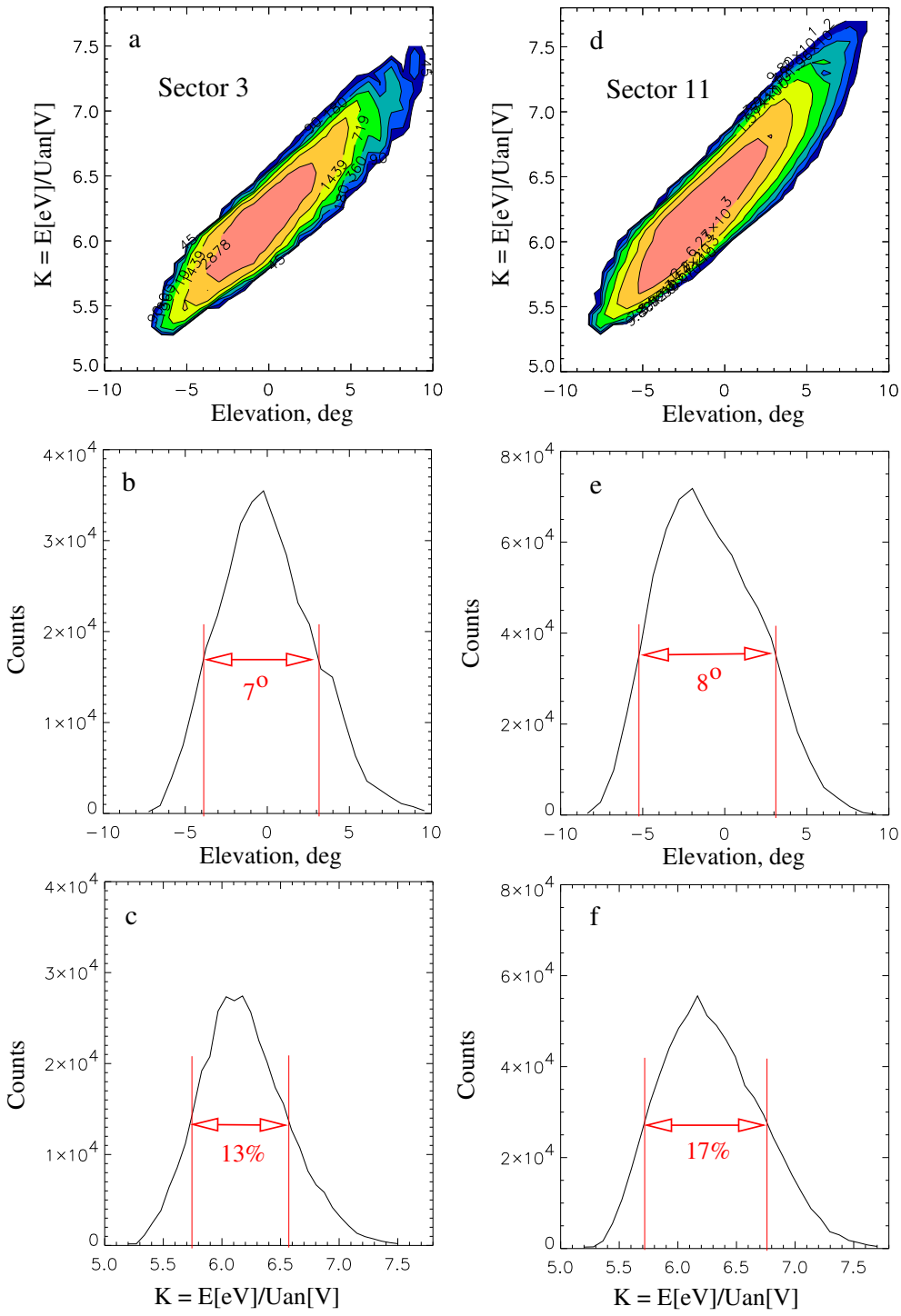

Figure 7: a,b,c: Sector 3 elevation - energy response when $Az = 14°$. d,e,f: the same for Sector 11 (without entrance grid), $Az = 5°$. The total count of sector 3 is 0.65 of total count of sector 11.

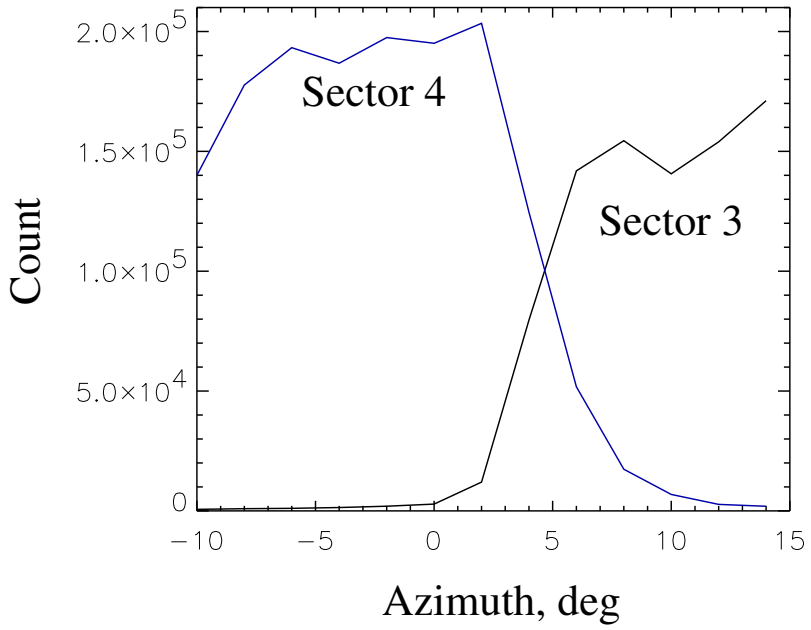

Figure 8: Azimuthal response of two next azimuthal sectors. Each point of the profile is the integral of energy-elevation response.

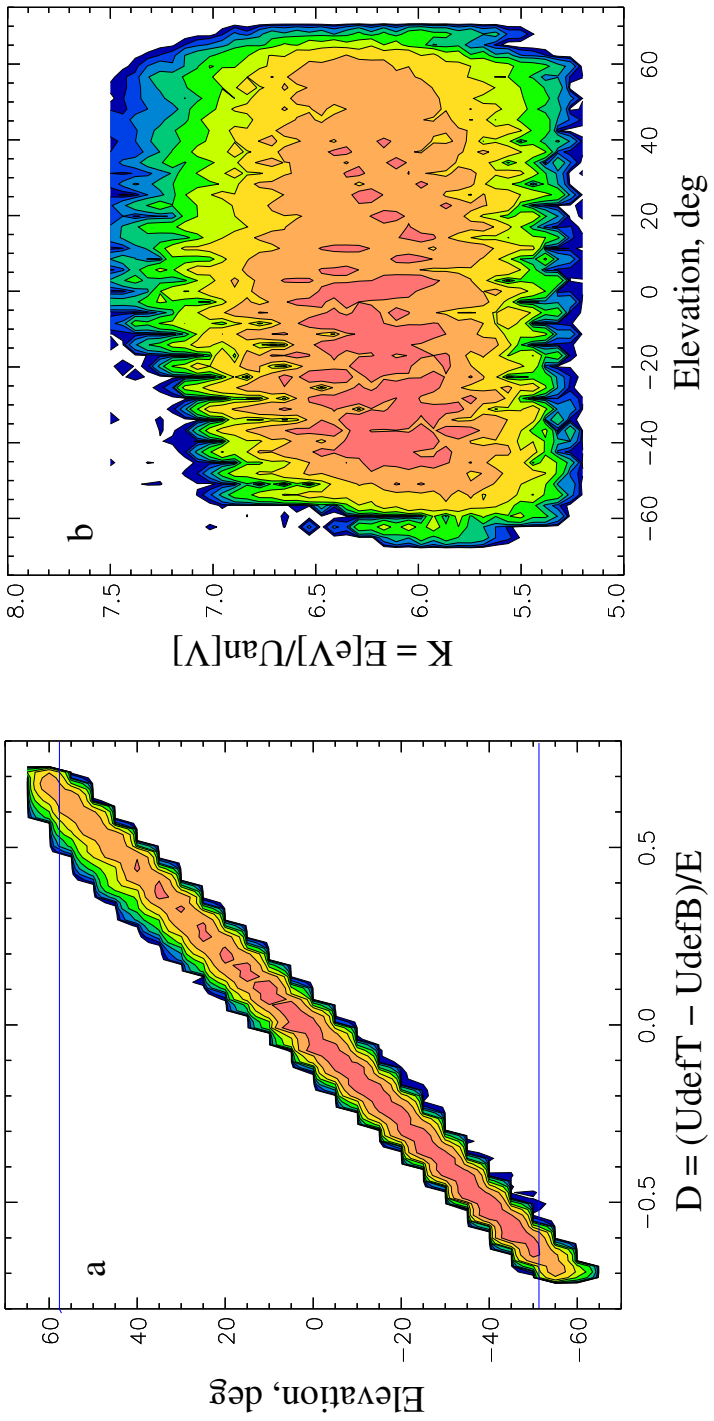

Figure 9: a: D - Elevation response. Two horizontal lines show limits of representative measurements. b: Re-calculated elevation K resopnse for whole elevation range.

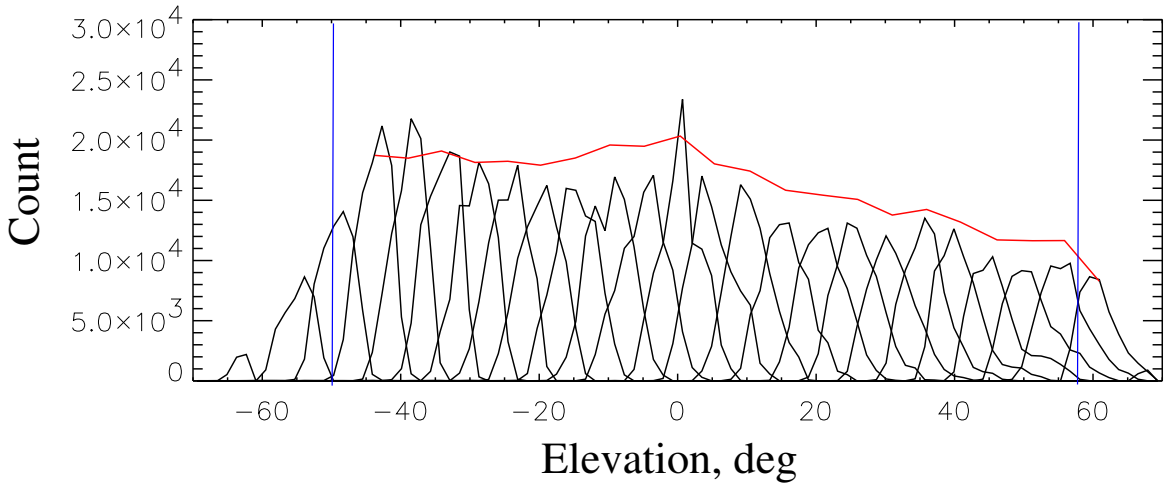

Figure 10: The recalculated elevation responses for 25 central elevation angles. Red line shows the profile of integral of each response.